

# Preclinical Evaluation of EC145, a Folate-*Vinca* Alkaloid Conjugate

Joseph A. Reddy, Ryan Dorton, Elaine Westrick, Alicia Dawson, Terri Smith, Le-Cun Xu, Marilyn Vetzal, Paul Kleindl, Iontcho R. Vlahov, and Christopher P. Leamon

Endocyte, Inc., West Lafayette, Indiana

## Abstract

We recently developed a new group of folate-conjugated *Vinca* alkaloids, one of which, EC145, emerged as a candidate for clinical development. Brief treatment of nude mice bearing ~100 mm<sup>3</sup> folate receptor-positive human xenografts led to complete response (CR) in 5/5 mice and cures (i.e., remission without a relapse for >90 days post-tumor implantation) in 4/5 mice. Multiple CRs and cures were also noted when EC145 was used to treat mice initially bearing tumors as large as 750 mm<sup>3</sup>. Likewise, complete cures (5/5) resulted following the treatment of an aggressive folate receptor-positive J6456 lymphoma model. The activity of EC145 was not accompanied by noticeable weight loss or major organ tissue degeneration. Furthermore, no significant antitumor activity (0/5 CR) was observed in EC145-treated animals that were co-dosed with an excess of a benign folate ligand, thus demonstrating the target-specific activity of EC145. The enhanced therapeutic index due to folate conjugation was also evidenced by the fact that the unconjugated drug (desacetylvinblastine monohydrate) was found to be completely inactive when administered at nontoxic dose levels and only marginally active when given at highly toxic dose levels. Subsequent dose regimen studies confirmed that EC145 given on a more frequent, qdx5 schedule resulted in the most effective antitumor response as compared with an equivalent total dose given on thrice- or single-injection-per-week schedule. Taken together, these studies show that EC145 has significant antiproliferative activity and tolerability, thus lending support to an ongoing phase I trial for the treatment of advanced malignancies. [Cancer Res 2007;67(9):4434–42]

## Introduction

Anticancer drugs generally affect all types of rapidly proliferating cells, and consequently, their therapeutic indices are narrow. Severe side effects are often observed, and clinical doses are more or less empirically determined by the risk of severe toxicity. In an effort to enhance the selectivity of a drug and simultaneously reduce unwanted toxicity (i.e., improving the therapeutic index), we and others have been developing tumor-targeted agents that display enhanced tumor-specific cell killing relative to their unconjugated drug counterparts. For example, Mylotarg is a monoclonal antibody (MAb)-drug conjugate that was approved for the treatment of acute myeloid leukemia, and it represents the first antibody-targeted drug conjugate on the market (1, 2). Likewise, many alternative antibody-drug conjugates are currently being tested

clinically (3, 4), and some will no doubt find their way to the marketplace. Due to their large molecular size of ~150,000 Da, MAbs typically clear from the blood and the body much more slowly compared with small-molecular-weight agents, a consequence that could lead to significant and unwanted drug exposure to normal organs. Some immunoglobulin G (IgG) molecules also show relatively poor diffusion from the vasculature and into tumors (5). Hence, we have hypothesized that replacing the MAb targeting ligand with a smaller but high affinity receptor-targeting ligand (e.g., folate) could possibly improve blood clearance and also enable better tumor penetration of attached drugs.<sup>1</sup>

The vitamin folate has been successfully used to deliver numerous therapeutic- and imaging-based agents to cells that express the folate receptor (FR) protein (6–10). The FR is a high-affinity membrane protein ( $K_d \sim 0.1$ – $1$  nmol/L for folic acid) that is functionally expressed in high quantities by many primary and metastatic cancers (11–13); and it has been successfully exploited for drug delivery purposes using a wide range of drug payloads (6–10, 14–22). We have previously described the biological activity of EC145, a novel folate conjugate of the powerful microtubule-destabilizing agent, desacetylvinblastine monohydrate (DAVLBH; a derivative of the natural product vinblastine).<sup>2</sup> Like vinblastine, DAVLBH is a *Vinca* alkaloid that is capable of disrupting the formation of the mitotic spindle, thereby inhibiting cell division and causing cell death. EC145, the water soluble folate conjugate of DAVLBH, was found to produce marked antitumor effect against FR-positive tumors using well tolerated regimens.<sup>2</sup> Herein, we report on our continued *in vivo* preclinical investigation of EC145, with particular emphasis on target specificity, efficacy toward large s.c. tumors, and optimized dosing regimens.

## Materials and Methods

**Materials.** Pteric acid (Pte) and *N*<sup>10</sup>-trifluoroacetyl-Pte were prepared according to Xu et al. (23). Peptide synthesis reagents were purchased from NovaBiochem and Bachem. EC145 was synthesized as previously described (24). EC20 (FolateScan; Pte-D- $\gamma$ Glu- $\beta$ Dpr-Asp-Cys) was prepared as previously described (25). Rhodamine isothiocyanate was purchased from Aldrich. All other common reagents were purchased from Sigma or other major suppliers.

**Synthesis, purification and analytic characterization of EC0260 and EC58.** The D-enantiomer of EC145, EC0260, was prepared by the same procedure as for EC145 with the exception that D-configured amino acid derivatives were used in the process. The final conjugates were purified by preparative high-performance liquid chromatography (HPLC; Waters NovaPak C<sub>18</sub> 19  $\times$  300 mm) with 1 mmol/L phosphate buffer (pH, 7.0; solvent A) and acetonitrile (solvent B) using a gradient consisting of 10% B to 50% B over 30 min at a flow rate of 15 mL/min. Acetonitrile was removed from the collected fractions *in vacuo*, and the residues were subjected

**Requests for reprints:** Christopher P. Leamon, Endocyte Inc., 3000 Kent Avenue, Suite A1-100, West Lafayette, IN 47906. Phone: 765-463-7175; Fax: 765-463-9271; E-mail: Chrisleamon@endocyte.com.

©2007 American Association for Cancer Research.  
doi:10.1158/0008-5472.CAN-07-0033

<sup>1</sup> J.A. Reddy, E. Westrick, H.K. Santhapuram, et al. Folate receptor specific antitumor activity of a folate-maytansinoid conjugate: submitted for publication.

<sup>2</sup> C.P. Leamon, J.A. Reddy, I.R. Vlahov, et al. Comparative preclinical activity of the folate-*Vinca* alkaloid conjugates EC140 and EC145. *Int J Cancer*. In press 2007.

to freeze-drying to give yellow amorphous solids. Liquid chromatography-mass spectrometry (LC-MS) data [ESI: (M + H)<sup>+</sup> = 1,918] and <sup>1</sup>H-nuclear magnetic resonance (<sup>1</sup>H-NMR) signals were in agreement with the proposed structures for EC145 and EC0260. In brief, the <sup>1</sup>H-NMR spectrum of each compound (300 MHz, D<sub>2</sub>O) contains 11 aromatic signals in the range from 6.4 to 8.8 ppm (five from the folate moiety and six from DAVLBH moiety). The signals for the two olefinic protons in DAVLBH appear at 5.5 ppm (d) and 5.7 ppm (m).

EC58 was prepared as follows. The folate-containing spacer unit N<sup>10</sup>-trifluoroacetyl-Pte-DγGlu-DγGlu-Lys-OH was synthesized using standard fluorenylmethyloxycarbonyl-based solid-phase peptide synthesis (Fmoc SPPS) on a Wang-resin polymeric support. It was purified by preparative HPLC (Waters NovaPak C<sub>18</sub> 19 × 300 mm) with 10 mmol/L NH<sub>4</sub>OAc (pH, 5; solvent A) and acetonitrile (solvent B) using a gradient consisting of 1% B to 20% B over 40 min at a flow rate of 15 mL/min. The structure of this compound was confirmed by LC-MS [ESI: (M + H)<sup>+</sup> = 795]. About 67 mg (85 μmol) of N<sup>10</sup>-trifluoroacetyl-Pte-DγGlu-DγGlu-Lys-OH were dissolved in 1.0 mL of DMSO, and to the well-stirred solution were added 50 mg (93 μmol) of rhodamine isothiocyanate and 30 μL (170 μmol) of *N,N*-diisopropylethylamine. The reaction mixture was stirred at room temperature for 6 h. DMSO was removed by freeze drying, and the crude product was reconstituted in 1 mmol/L NH<sub>4</sub>HCO<sub>3</sub> (solvent A) for 30 min at room temperature, followed by preparative HPLC purification [Waters NovaPak C<sub>18</sub> 19 × 300 mm column with solvent A and acetonitrile (solvent B) using a gradient consisting of 1% B to 50% B over 60 min at a flow rate of 15 mL/min]. LC-MS [ESI: (M + H)<sup>+</sup> = 1,142; (M - H)<sup>+</sup> = 1,140] was in agreement with the expected structure.

**In vivo antitumor experiments.** Four- to six-week-old female *nu/nu* mice (Charles River) or six- to seven-week-old female BALB/c mice (Harlan Sprague-Dawley, Inc.) were maintained on a standard 12-h light-dark cycle and fed *ad libitum* with folate-deficient chow (Harlan diet TD00434; Harlan Teklad) for the duration of the experiment. Because normal rodent chow contains a high concentration of folic acid (6 mg/kg chow), mice used in these studies were maintained on the folate-free diet for 2 weeks before tumor implantation to reduce serum folate concentrations from an initial average of 720 to ~25 nmol/L, which is close to the range of normal human serum (9–14 nmol/L; ref. 26). FR-positive human nasopharyngeal KB cells (~75 pmol FR/mg protein; ref. 27; American Type Culture Collection) and J6456 murine lymphoma cells were grown continuously as a monolayer or in suspension, respectively, using folate-free RPMI containing 10% heat-inactivated FCS (HIFCS) at 37°C in a 5% CO<sub>2</sub>/95% air-humidified atmosphere with no antibiotics. The HIFCS contains endogenous folates at concentrations sufficient for FR-expressing cells to survive and proliferate in this medium (14), which consequently is more physiologically relevant than typical cell culture media, which contain 100- to 1,000-fold higher levels of folates. KB cells (1 × 10<sup>6</sup> per *nu/nu* mouse) or J6456 cells (1 × 10<sup>6</sup> per BALB/c mouse) in 100 μL were injected in the subcutis of the dorsal medial area. Mice were divided into groups of five, and test articles were freshly prepared and injected through the lateral tail vein under sterile conditions in a volume of 200 μL of PBS. I.v. treatments were typically initiated on day 9 post-tumor cell implantation when the KB tumors were ~70 to 110 mm<sup>3</sup> in volume, and on day 19 post-tumor cell inoculation (PTI) when the J6456 tumors were ~100 to 160 mm<sup>3</sup> in volume. In the large KB tumor study, mice were dosed 13 days PTI in the 250-mm<sup>3</sup> group, 20 days PTI in the 500-mm<sup>3</sup> group, and 24 days PTI in the 750-mm<sup>3</sup> group. The mice in the control groups received no treatment. Growth of each s.c. tumor was followed by measuring the tumor thrice per week (TIW) during treatment and twice per week thereafter until a volume of 1,500 mm<sup>3</sup> was reached. Tumors were measured in two perpendicular directions using Vernier calipers, and their volumes were calculated as 0.5 × *L* × *W*<sup>2</sup>, where *L* = measurement of longest axis in millimeters and *W* = measurement of axis perpendicular to *L* in millimeters. As a general measure of toxicity, changes in body weights were determined on the same schedule as tumor volume measurements. Survival of animals was monitored daily. Animals that were moribund (or unable to reach food or water) were euthanized by CO<sub>2</sub> asphyxiation. All *in vivo* studies were done in accordance with the American Accreditation Association of Laboratory Animal Care guidelines.

Drug toxicity was assessed by collecting blood via cardiac puncture and submitting the sera and whole blood for independent analysis of serum chemistry and hematologic parameters at Ani-Lytics, Inc. In addition, histopathologic evaluation of formalin-fixed heart, lungs, liver, spleen, kidney, intestine, skeletal muscle, and bone (tibia/fibula) were done at Animal Reference Pathology Laboratories.

**Tumor response criteria.** For individual tumors, a partial response (PR) was defined as volume regression >50% but with measurable tumor (>2 mm<sup>3</sup>) remaining at all times. Complete response (CR) was defined as a disappearance of measurable tumor mass (<2 mm<sup>3</sup>) at some point within 90 days after tumor implantation. Cures were defined as CRs without tumor regrowth within the 90-day study time frame.

**FolateScan (<sup>99m</sup>Tc-EC20) uptake in BALB/c mice bearing M109 tumors.** An EC20 kit was used for the preparation of radioactive drug substance (25). Each kit contains a sterile, nonpyrogenic lyophilized mixture of 0.1 mg of EC20, 80 mg of sodium α-D-glucoheptanate dihydrate, 80 μg of tin(II) chloride dihydrate, and sufficient sodium hydroxide or hydrochloric acid to adjust the pH to 6.8 ± 0.2. Chelation of <sup>99m</sup>Tc to EC20 was done by injecting 1 mL of sodium pertechnetate <sup>99m</sup>Tc injection (<50 mCi) into this vial and heating it for ~18 min in a boiling water bath. Samples of the <sup>99m</sup>Tc-EC20 solution were analyzed for radiochemical purity using a HPLC system consisting of a Waters 600E Multisolvent Delivery System and 490 UV detector, a Bioscan FC-3200 radiodetector, Laura v1.5 radiochromatogram software, and a Waters Nova-Pak C18 (3.9 × 150 mm) column. Injected samples were eluted isocratically using an aqueous mobile phase containing 20% methanol and 0.1% trifluoroacetic acid at a flow rate of 1 mL/min. The radiochemical purity of <sup>99m</sup>Tc-EC20 was >90% (25).

Female BALB/c mice (6–7 weeks of age) were maintained on a folate-free diet for a total of 4 weeks before the biodistribution experiment. Syngeneic, FR-positive murine lung adenocarcinoma tumor cells (M109; ~25 pmol FR/mg protein; 1 × 10<sup>6</sup> cells per animal) were inoculated in the subcutis of the dorsal medial area of the right axilla (27). Stock <sup>99m</sup>Tc-EC20 solutions containing 100 μg of agent per milliliter were prepared on the day of use. Mice with 200- to 500-mm<sup>3</sup> M109 tumors received a <sup>99m</sup>Tc-EC20 dose of 0.1, 0.3, 1, 3, or 10 μmol/kg in 200 μL sterile PBS via a tail vein. Four hours post-injection, animals were sacrificed by CO<sub>2</sub> asphyxiation and dissected. Tumors and livers were removed and weighed, and their radioactivity content was measured in an automatic gamma counter to determine <sup>99m</sup>Tc distribution. Uptake of the radiopharmaceutical, expressed as percent injected dose of wet weight tissue (% ID/g), was calculated by reference to standards prepared from dilutions of the injected preparation (20).

**Folate-rhodamine uptake into M109 tumors.** BALB/c mice bearing 400- to 600-mm<sup>3</sup> M109 tumors received 2 μmol/kg of EC58, a folate-rhodamine conjugate, or unconjugated rhodamine i.v. in 200 μL of PBS. One hour later, mice were euthanized by CO<sub>2</sub> inhalation, and tumors were harvested. Tumor slices (1 to 2 mm thick) were covered with Tissue Tek OCT compound and immediately frozen in liquid nitrogen. The tumor slices were frozen to -20°C and then sectioned (7 μm thick) using a Leica CM3050 Cryostat. The sections were counterstained with Hoechst 33258 (1.2 μg/mL) for 10 min. The tumor sections were mounted using anti-fade (Biomed) liquid mount and then imaged using a Leica DMLB fluorescent microscope.

## Results

**FR-specific *in vivo* potency of EC145.** Initial experiments were carried out in athymic nude mice bearing s.c. implanted, FR-expressing KB xenografts (70–110 mm<sup>3</sup>). In our lab, the human KB xenograft is a relatively quick-growing tumor that reproducibly displays log-linear growth and reaches a volume of about 1,500 mm<sup>3</sup> within ~30 days post s.c. tumor implantation (1 × 10<sup>6</sup> cells) on the back of female *nu/nu* mice. The activity of EC145 against this model was assessed by giving the drug 9 days PTI using a 2 μmol/kg dose level and following a TIW, 2-week schedule. As shown in Fig. 1B, EC145 generated remarkable antitumor effect where 5/5 animals displayed a CR, of which four of the five animals

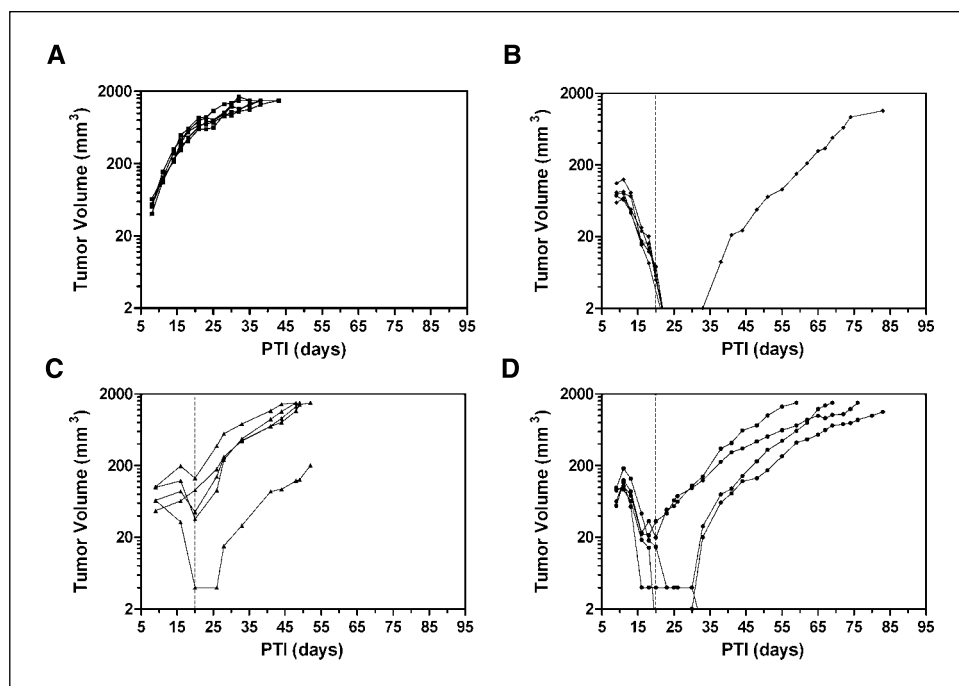


**Figure 1.** Comparison of the therapeutic efficacy of EC145 and EC0260 against s.c. FR-positive KB tumor growth. KB tumor cells ( $1 \times 10^6$ ) were inoculated s.c. into nude mice, and therapy started on randomized mice with tumors in the 70- to 110-mm<sup>3</sup> range. The therapeutic regimen consisted of i.v. doses of 2  $\mu$ mol/kg per injection following a TIW, 2-wk schedule. A, untreated controls; B, EC145; C, EC145 + 20 equivalents of EC20; D, EC0260. Each curve represents the growth of a single tumor in an individual mouse. The dotted vertical lines denote the final day of dosing.

maintained the CR (i.e., cures) throughout the 90-day duration of the study. In contrast, when co-dosed with a modest 20-fold molar excess of a benign water-soluble folate analogue (EC20), EC145 failed to produce any meaningful antitumor activity (zero CRs and two PRs; see Fig. 1C). This outcome indicated that the activity of EC145 was predominantly dependent on binding to tumor-associated FRs. Furthermore, EC145-treated animals did not lose any significant weight throughout the dosing period; and no durable tissue damage was observed upon histologic examination of liver, spleen, kidney, lung, and heart as done on animals euthanized 80 to 120 days after EC145 administration, which is consistent with our earlier report.<sup>2</sup>

EC145 is constructed with an all L-peptide spacer conjugated to the  $\gamma$ -carboxylic acid of folate's glutamyl residue (24). To better understand the importance of the stereochemical configuration of the linker with regard to its overall pharmacology, the all-D enantiomer (EC0260) was synthesized. We have previously reported that EC145 has a affinity of 0.47 relative to that of folic acid for human FRs.<sup>2,3</sup> When a similar assay was done on EC0260, the relative affinity was determined to be  $\sim 0.2$ . As shown in Fig. 1D, EC0260 was found to be less active against established KB tumors than EC145 by producing only two CRs, three PRs, and one cure. This lower observed therapeutic efficacy may have been due to the slightly reduced affinity of EC0260 for the FR. Regardless, the data in Fig. 1 collectively show that EC145 is the better agent for FR-targeted therapy.

**Antitumor effect of DAVLBH, the nontargeted form of EC145.** To better determine the approximate therapeutic range of the unconjugated DAVLBH drug, *nu/nu* mice bearing 70- to 110-mm<sup>3</sup> KB tumors were treated with three different doses (0.5, 1, and

2  $\mu$ mol/kg) of this agent following a TIW, 2-week regimen; tumor growth and body weight were subsequently monitored. As shown in Fig. 2A, antiproliferative activity was clearly absent when DAVLBH was dosed at a nontoxic level (0.5  $\mu$ mol/kg). When dosed with 1  $\mu$ mol/kg, DAVLBH produced minimal antitumor activity (zero CRs; five PRs) but caused weight loss of up to 14% (see Fig. 2B and D). In the high-dose 2  $\mu$ mol/kg cohort, mice could only be dosed thrice with DAVLBH before losing as much as 20% weight (Fig. 2C and D). These results are in stark contrast to that produced from DAVLBH's folate-targeted counterpart; because therapy with 2  $\mu$ mol/kg of EC145 produced 4/5 cures without any weight loss (compare Figs. 1 and 2). Unlike EC145, DAVLBH clearly seems to possess a very narrow therapeutic range.

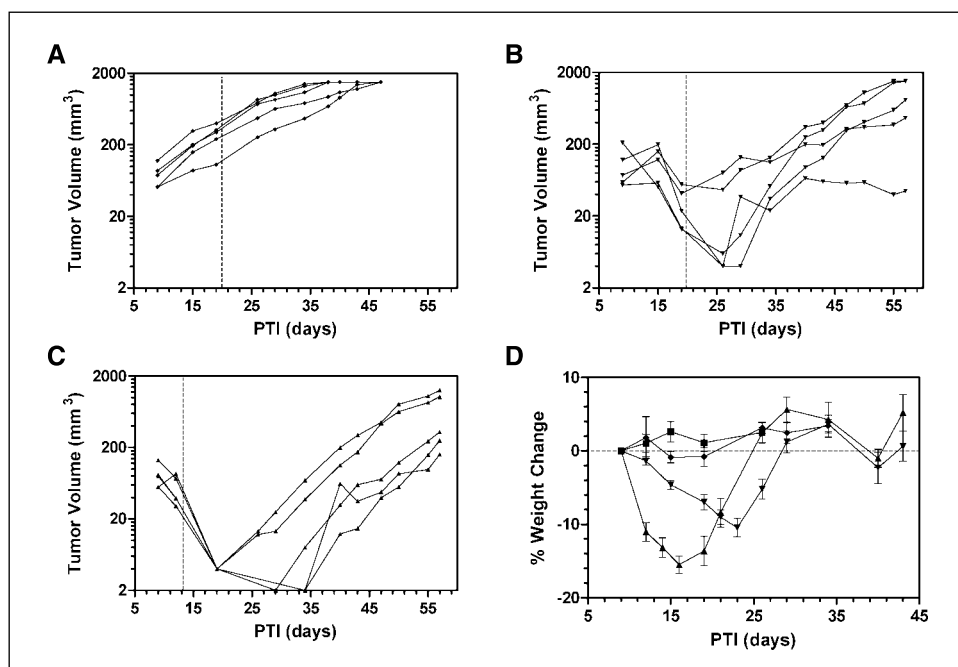
#### Antitumor activity against an aggressive lymphoma model.

EC145 was also tested for activity against an aggressive FR-positive J6456 lymphoma tumor model. Following the s.c. implantation of 1 million cells per animal, tumors typically reach a volume of 1,500 mm<sup>3</sup> within  $\sim 26$  days. Here, BALB/c mice bearing s.c. J6456 lymphoma tumors were treated with 2  $\mu$ mol/kg of EC145 TIW, for 2 consecutive weeks. As shown in Fig. 3B, tumors in all five treated mice had quickly regressed and did not relapse during the study period (i.e., 5/5 cures). EC145 therapy was also found to be well tolerated in the BALB/c mice, and its toxicity profile was similar to that observed in the *nu/nu* mice (see Fig. 3D). Together with the results shown in Fig. 1, EC145 seems to be a very effective agent for treating FR-positive tumors.

**EC145 can eradicate large, well-established KB tumor xenografts.** In an attempt to relate tumor size with the antitumor efficacy of EC145, we dosed mice with 2  $\mu$ mol/kg of EC145, TIW for 3 consecutive weeks beginning when the tumor volumes measured 250, 500, or 750 mm<sup>3</sup>. In the 250-mm<sup>3</sup> group, treatment with EC145 produced CRs in four of five mice within 14 to 21 days from the initiation of therapy, and three of these animals were presumed to be cured (Fig. 4B). In the 500-mm<sup>3</sup> group, EC145 continued to provide a strong therapeutic effect with two CRs and three PRs, of

<sup>3</sup> As has been observed with other folate conjugates, such as folate-mitomycin (28), we expect this high level of affinity to be maintained with mouse FRs.

**Figure 2.** Antitumor effects of nontargeted DAVLBH and its toxicity toward the treated *nu/nu* mice. KB tumor cells ( $1 \times 10^6$ ) were inoculated s.c. into nude mice, and therapy started on randomized mice with tumors in the 70- to 110- $\text{mm}^3$  range. The therapeutic regimen consisted of i.v. doses of DAVLBH on a TIW schedule for 2 wks. A, 0.5  $\mu\text{mol/kg}$  per injection; B, 1  $\mu\text{mol/kg}$  per injection; C, 2  $\mu\text{mol/kg}$  per injection; each curve represents the growth of a single tumor in an individual mouse. D, points, average weights of five mice for each treatment cohort; bars, SD. ■, control; ◆, 0.5  $\mu\text{mol/kg}$  per injection; ▼, 1  $\mu\text{mol/kg}$  per injection; ▲, 2  $\mu\text{mol/kg}$  per injection. The dotted vertical lines denote the final day of dosing.

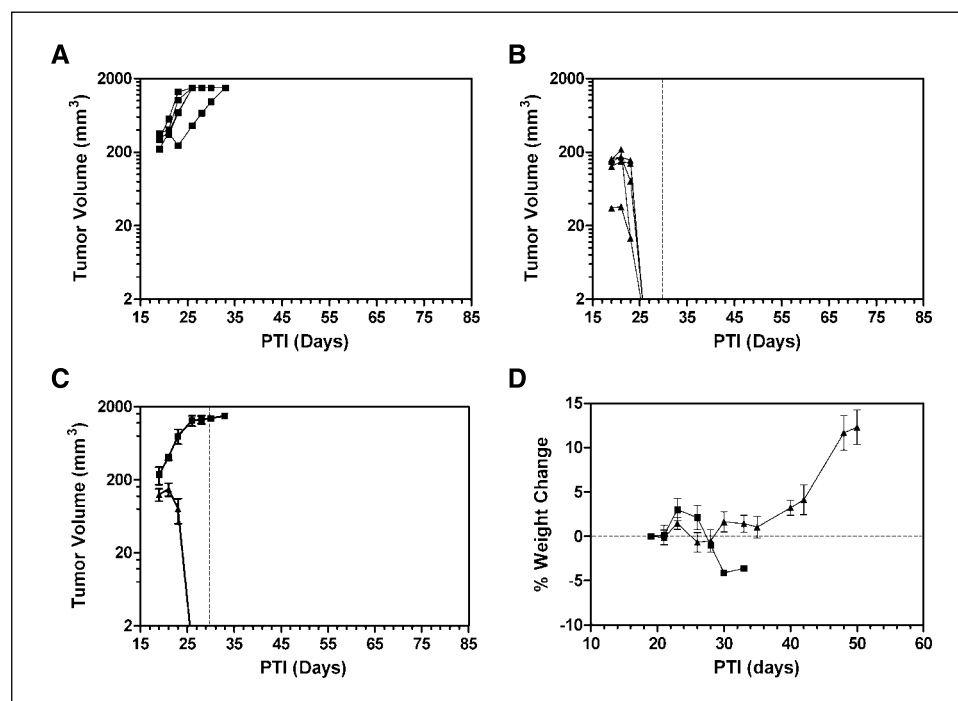


which one animal was cured (Fig. 4C). Remarkably, antitumor efficacy was strong even against the largest sized tumors (750- $\text{mm}^3$  tumors), where two CRs, three PRs, and two cures were observed (Fig. 4D). Interestingly, at the end of the 3-week treatment, the tumor regrowth rate in two of the three relapsed mice from this latter group was considerably slower than control tumor growth rates.

**Intratumoral accessibility of folate conjugates.** The data in Fig. 4 clearly indicate that EC145 can produce meaningful anti-

tumor effect against very large s.c. tumors. However, it did seem that the net activity decreased with the size of tumor. We questioned whether this compromised activity was the result of ending therapy too soon, or was it due to inefficient cellular targeting within such large malignant masses. To address the latter issue, nude mice bearing large 500- $\text{mm}^3$  KB tumors were injected i.v. with 2  $\mu\text{mol/kg}$  of EC58, a folate-rhodamine conjugate. One hour postinjection, mice were sacrificed; their tumors were excised, frozen in liquid nitrogen, and

**Figure 3.** Effect of EC145 against FR-positive J6456 lymphoma tumors. J6456 tumor cells ( $1 \times 10^6$ ) were inoculated s.c. into BALB/c mice, and therapy started for randomized mice with tumors in the 50- to 100- $\text{mm}^3$  range. The therapeutic regimen consisted of i.v. doses of EC145 on a 2  $\mu\text{mol/kg}$  per injection, TIW schedule for 2 consecutive weeks. A, untreated J6456 controls; B, EC145; each curve represents the growth of a single tumor in an individual mouse. C and D, points, average volume of five tumors and the average weights of five mice, respectively, for each treatment cohort; bars, SD. ■, control; ▲, EC145. Dotted vertical lines, final day of dosing.



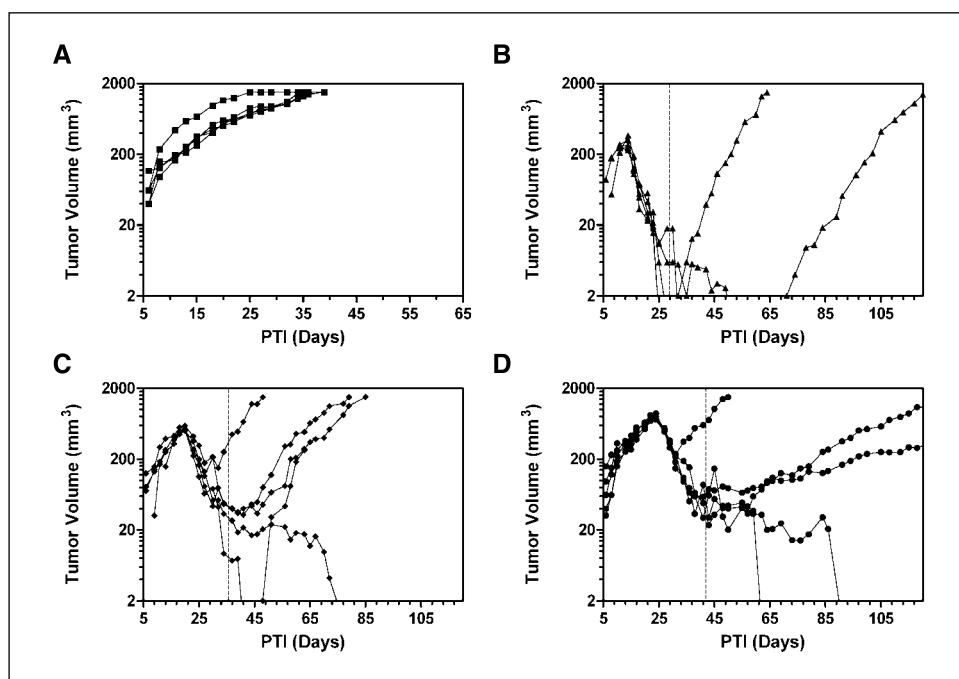


**Figure 4.** Effect of EC145 on large established KB tumors. KB tumor cells ( $1 \times 10^6$ ) were inoculated s.c. into nude mice, and therapy started when tumors reached an average predetermined range. The therapy regimen consisted of i.v. doses of  $2 \mu\text{mol/kg}$  per injection following a TIW, 3-wk schedule. A, untreated controls; B,  $250 \text{ mm}^3$ ; C,  $500 \text{ mm}^3$ ; D,  $750 \text{ mm}^3$ ; each curve represents the growth of a single tumor in an individual mouse. Dotted vertical lines, final day of dosing.

then sectioned for fluorescence microscopy. As shown in Fig. 5B, tumor cells in these microscopic sections, both at the center and periphery of the tumor, were first identified by *ex vivo* nuclear staining with Hoechst 33258 (*blue fluorescence*). Imaging of these sections in the same optical field for rhodamine fluorescence revealed that all of the tumor cells in the center as well as the periphery had been uniformly stained with EC58 (Fig. 5A). As a

control for specificity, Fig. 5C shows that KB tumors in mice injected with unconjugated rhodamine did not significantly emit fluorescence. These data confirm that all of the tissue throughout a large tumor is readily accessible to a small-molecular-weight folate-conjugate, thereby suggesting that more durable antitumor responses might be feasible with continued therapy (see Discussion).

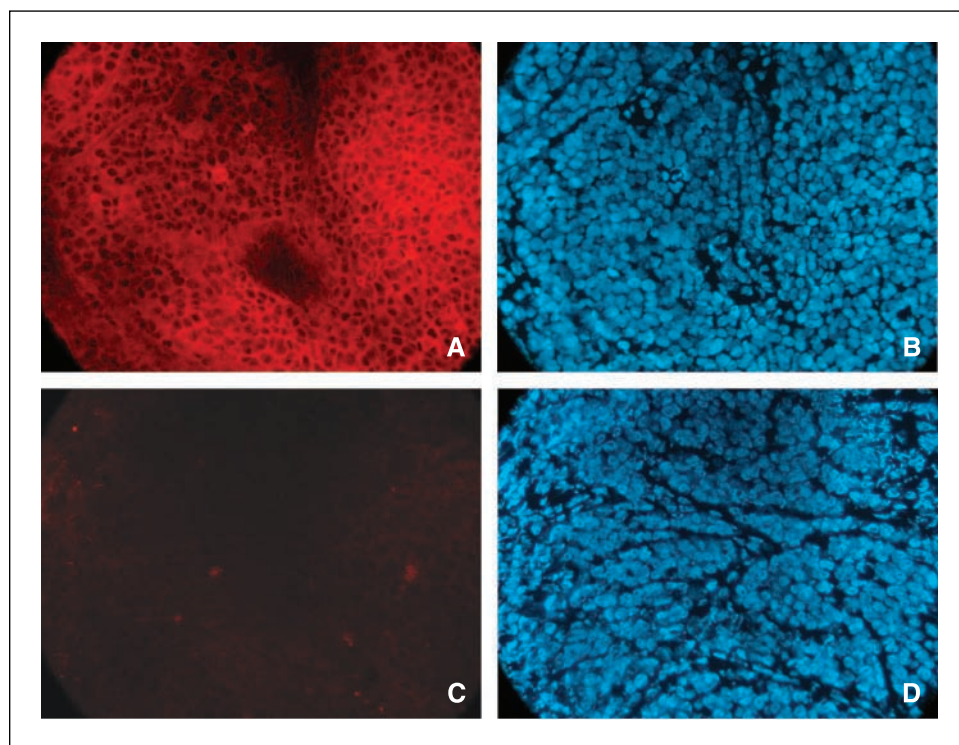
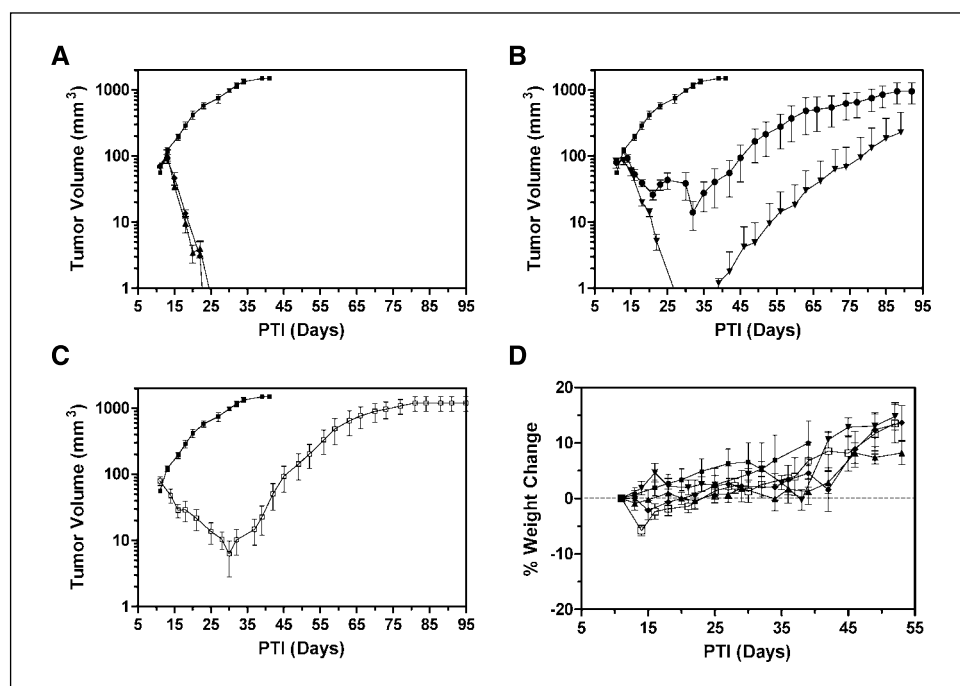


**Figure 5.** Uptake of folate-rhodamine into large ( $500\text{-mm}^3$ ) s.c. KB tumors. One hour after i.v. injection of  $2 \mu\text{mol/kg}$  EC58 (folate-rhodamine), tumor cell uptake was detected throughout the tumor (A). C, fluorescence of a KB tumor in mice injected with unconjugated rhodamine. B and D, corresponding Hoechst 33258 nuclear staining of the identical tissue sections from A and C, respectively.

**Figure 6.** Effect of treatment schedule on the antitumor efficacy and weight loss due to EC145 therapy. Randomized *nu/nu* mice with KB tumors (50–100-mm<sup>3</sup> range) were treated with EC145 at various doses and schedules. **A**, ■, control; ▲, 1.2  $\mu\text{mol/kg}$  per injection, qdx5 for 2 consecutive weeks; ◆, 1.2  $\mu\text{mol/kg}$  per injection, qdx5 in the first and third weeks; **B**, ■, control; ▼, 2  $\mu\text{mol/kg}$  per injection, TIW for 2 consecutive weeks; ●, 2  $\mu\text{mol/kg}$  per injection, TIW in the first and third weeks; **C**, ■, control; □, 4  $\mu\text{mol/kg}$  per injection, SIW for 3 consecutive weeks. *Points*, average volume of five tumors; *bars*, SD. **D**, *points*, weights of five mice for each of the above treatment cohort; *bars*, SD.



**Optimization of EC145 treatment schedule.** Animal models allow for the investigation of a range of dose levels and schedules to help guide clinical investigation. Hence, to get a better idea on the effect of dose and schedule on the efficacy and toxicity of EC145, mice were treated with a fixed amount of this agent (12  $\mu\text{mol/kg}$  total) spread out over a 3-week period and dosed according to varied but defined regimens. The following doses and schedules were used: (a) 1.2  $\mu\text{mol/kg}$ , qdx5 for 2 consecutive weeks; (b) 1.2  $\mu\text{mol/kg}$ , qdx5 during weeks 1 and 3; (c) 2  $\mu\text{mol/kg}$ , TIW for 2 consecutive weeks, (d) 2  $\mu\text{mol/kg}$ , qdx5 during weeks 1 and 3; and (e) 4  $\mu\text{mol/kg}$ , single injection per week (SIW) for 3 consecutive weeks. As shown in Fig. 6A, both qdx5 regimens produced 100% cures; thus, having the second week off from therapy did not adversely impact response when the agent was administered daily. Furthermore, when gross and histopathologic examinations were done, none of these treated mice showed any signs of tumor at the end of the study (92 days). Administration of EC145 on a TIW schedule was found to be somewhat less active; but more importantly, having 1 week of rest in between the dosing period was found to significantly compromise the therapeutic effect when dosed according to this less frequent schedule. For instance, EC145 given TIW for 2 consecutive weeks produced four of five cures with one PR, whereas EC145 given TIW every other week yielded two CRs, three PRs, and only one cure (Fig. 6B). The latter regimen was found to be comparable to the 4  $\mu\text{mol/kg}$ , SIW 3-week regimen, where two CRs, three PRs, and one cure were noted (Fig. 6C). Importantly, none of these dosing regimens resulted in significant toxicity to the treated mice (Fig. 6D). From these results, it was concluded that a dose-dense, daily administration (qdx5) of EC145 was superior to all of the less frequent dosing regimens.

**Rationale for dose-dense regimens.** In an attempt to relate the surprisingly high antitumor effect produced by administering EC145 more frequently at lower dose levels to the quantitative tumor uptake of folate conjugates, BALB/c mice bearing FR-

positive M109 tumors were dosed with increasing amounts of <sup>99m</sup>Tc-EC20 (Folate-Scan; refs. 20, 25, 29) and then sacrificed 4 h later to measure the uptake of this radiodiagnostic agent in tumor (target tissue; ~25 pmol FR/mg protein) and liver (nontarget tissue; ~0.1 pmol FR/mg protein; ref. 27). <sup>99m</sup>Tc-EC20 is a well-known, small-molecular-weight, folate-based agent that readily binds to FR-positive tissue following i.v. administration (20, 25); this agent is also currently being used in the clinic for determining patient eligibility for experimental folate-targeted therapies (Endocyte, Inc.).

As shown in Table 1A, <sup>99m</sup>Tc-EC20 uptake in liver (L) tissue increased rather proportionally to the dose administered, but the uptake in the tumor (T) was apparently saturated at bolus dose levels >3  $\mu\text{mol/kg}$ . The tumor-to-liver uptake ratios (T/L) at each dose are also summarized in Table 1A. The T/L ratio peaked at a dose of ~0.3  $\mu\text{mol/kg}$ , above which there was a disproportionate increase in the liver uptake as compared with that in the tumor. Using the dose levels applied in the aforementioned schedule study (Fig. 6) and the values in Table 1A, we estimated the T and L uptake levels provided by a single EC145 dose and then calculated the total uptake that these tissues could have experienced for each evaluated regimen. For example, 2.5% of a single 1.2  $\mu\text{mol/kg}$  EC145 dose was estimated to be captured per gram of tumor or a total of 25.4% ID/g over the entire 10-dose regimen (i.e., qdx5, 2 weeks). As summarized in Table 1B, tumor uptake was found to be significantly greater when EC145 was administered at lower dose levels but following a more frequent schedule (contrast 25.4% versus 12.3% net uptake for the qdx5 and SIW regimens, respectively). Importantly, this drop in tumor uptake could easily explain the observed reduction in the antitumor effect of EC145 when dosed using the less frequent, higher dose level regimens (see Fig. 6). The T/L ratio was also greatest when EC145 was administered daily. Curiously, total liver uptake was found to be less affected by the dose and schedule perhaps because this organ is involved in the clearance of folate conjugates via a

**Table 1.**(A) Tumor (T) and liver (L) uptake and T/L tissue ratios from M109 tumor-bearing BALB/c mice injected with <sup>99m</sup>Tc-EC20

Dose (μmol/kg)	Uptake (% ID/g)		Liver	T/L ratio
	Tumor			
0.1	0.36 ± 0.03		0.12 ± 0.07	2.97
0.3	0.95 ± 0.15		0.47 ± 0.43	4.59
1	2.23 ± 0.57		0.65 ± 0.04	3.41
3	3.8 ± 0.38		1.64 ± 0.39	3.1
10	4.81 ± 0.63		4.19 ± 1.07	1.42

(B) Estimated cumulative tumor (T) and liver (L) uptake of a folate conjugate when dosed following various schedules

Regimen			Tissue uptake per dose (% ID/g)		Total tissue uptake per cycle (% ID/g)		T/L ratio
Dose level (μmol/kg)	Schedule	Total dose (μmol/kg)	Tumor	Liver	Tumor	Liver	
1.2	qdx5, 2 wks	12.0	2.5	0.7	25.4	7.3	3.5
2.0	TIW, 2 wks	12.0	3.2	1.2	19.5	7.1	2.8
4.0	SIW, 3 wks	12.0	4.1	2.1	12.3	6.4	1.9

NOTE: % ID/g, percent injected dose per gram of wet weight tissue. Values in (A) are the means ± SD (n = 3).

non-FR-mediated mechanism.<sup>4</sup> Overall, these data clearly show that folate-targeted agents may be best administered following more frequent dosing regimens.

**Preliminary toxicity assessment.** Aside from minimal weight loss during EC145 therapy, no other obvious gross toxicities were observed.<sup>2</sup> Formal Good-Laboratory-Practice toxicology studies have been completed with EC145 in both rodents and dogs to support the filing of an Investigational New Drug application. Particular findings that defined the maximum tolerated dose were related to proliferative compartment toxicities, such as the gastrointestinal tract and the hematopoietic system.<sup>4</sup> However, all toxicities were declared to be reversible.

## Discussion

In this report, we provide additional evidence that EC145, a folate-conjugated *Vinca* alkaloid, produces a highly potent and specific antitumor effect against FR-expressing tumors in *nu/nu* and BALB/c mice. Following brief cycles of therapy, tumors were repeatedly observed to shrink, often without recurrence, when using regimens that produced little if any noticeable weight loss or adverse events. The fact that such effects were seen in multiple FR-positive models (including the M109 model previously reported)<sup>2</sup> suggests that EC145 may be a useful agent in the fight against some human cancers.

Initial studies in mice suggested that EC145 was more potent and far less toxic than its unconjugated drug counterpart, DAVLBH.<sup>2</sup> To confirm our earlier findings and using a direct comparison approach, tumor-bearing animals received increasing

amounts of DAVLBH according to a TIW, 2-week schedule (i.e., a regimen known to be very efficacious and well tolerated for EC145). Importantly, no activity was observed when DAVLBH was dosed at a seemingly nontoxic level (0.5 μmol/kg), and only PRs were noted at the 1 μmol/kg maximum tolerated level, where mice lost ~14% of their weight. In our animal model, DAVLBH was not tolerable at the 2 μmol/kg level when given more than thrice. Unlike EC145, DAVLBH obviously has a very narrow therapeutic index.

Increased tumor burden is usually associated with reduced chemotherapeutic efficacy. One plausible explanation for this effect is that the tumor cells located further away from the nearest capillary are actually less accessible to parenterally administered drugs. Although EC145 is a targeted agent, its ability to access tumor cells is still presumably governed by the laws of extravascular diffusion; however, compared with its untargeted drug counterpart, EC145 has the distinct advantage of docking to the tumor cells and being endocytosed by virtue of the high-affinity FR. To directly address the performance of EC145 against larger tumors, we delayed the onset of therapy to animals until their tumors were 250, 500, or 750 mm<sup>3</sup> in volume. Here, we observed strong antitumor responses among all three cohorts, including 2/5 cures in the largest 750-mm<sup>3</sup> tumor group. These results suggested that even as the tumor increased in size, the cells within the malignant mass remained accessible to folate conjugates, like EC145. To confirm that hypothesis, mice bearing large s.c. tumors were injected with a fluorescent folate-rhodamine conjugate, and bright fluorescence was observed to be uniformly diffused throughout the tumor. In other words, all tumor cells within the large malignant mass seemed to be labeled and, hence, readily accessible to the systemically administered folate-targeted agent. These findings are consistent with a previous report from our group which showed that FR-targeted <sup>99m</sup>Tc-EC20 tumor uptake

<sup>4</sup> C. Leamon et al., in preparation.

increased proportionally to the size of the tumor (20). Taken together, these data provide optimism that small-molecular-weight, folate-targeted agents may be useful for treating patients with large, inoperable tumor burden. Furthermore, because the treated animals did not experience any observable adverse effects during therapy, it may also be possible to obtain more pronounced antitumor activity with EC145 by simply extending the duration of treatment. Although extended i.v. dosing regimens are typically difficult to conduct with mice, such manipulations would be feasible at the clinical level.

The preclinical phase of drug development provides an excellent opportunity to evaluate the effect of dosage and treatment schedules on therapeutic efficacy. Admittedly, an optimal treatment regimen defined for mice may not directly translate to success in the clinic; but because little is known about the translation of folate-targeted therapeutics, our laboratory elected to study the effects of altering the dosing regimen on the performance of EC145 in mice with the hopes of providing some guidance to clinicians. In fact, we were curious whether a dose-dense (metronomic) approach would be useful in the setting of folate-targeted therapy simply because it seemed sensible to maximize FR loading with EC145 by dosing this agent more frequently. Our approach reported above tested the effects of administering a fixed total quantity of EC145 (12  $\mu\text{mol/kg}$ ) spread over a 3-week period. Of the three schedules evaluated (qdx5, TIW, and SIW), EC145 was found to be most efficacious (100% cures) against FR-positive tumors when administered at low, but more frequent (qdx5) doses; furthermore, EC145 was determined to be least effective when given at high, less frequent doses. Curious about these findings, we examined the dose-dependent biodistribution profiles of  $^{99\text{m}}\text{Tc}$ -EC20 (FolateScan; a folate-drug surrogate) and found that the reduced activity observed with less frequent, higher dose regimens of EC145 could possibly be explained by a nonlinear tumor uptake property (due to the receptor saturating phenomenon; see Table 1A). Theoretical calculations suggested that the total drug uptake in the tumor following the qdx5 regimen could have been 30% greater than with the TIW schedule and  $\sim 100\%$  greater than with the SIW regimen. Given the steep dose-response curves for many chemotherapeutic agents, these

increases in tumor uptake of the drug are significant and should translate into improvements of therapeutic efficacy. Interestingly, FolateScan uptake in liver (a FR-negative, nontargeted organ; ref. 27) increased linearly and was proportional to the administered dose. Consequently, one might predict that a less frequent, larger dose regimen may not only result in lower antitumor effect, but also a corresponding increase in toxicity. With these data, we believe that the choice of administration schedule may be more important for folate-targeted therapeutic agents than simply increasing the dose level. Admittedly, we do recognize that more frequent treatment schedules mean that both patients and clinicians will be encumbered with more responsibility and workload. However, compliance for such approaches might actually be high if response rates are shown to increase, and toxicities are determined to be low or easily managed.

Preliminary pharmacokinetic analysis of EC145 has shown that it has a serum half life of  $\sim 1.3$  min in mice. Similar rapid tissue distribution and elimination phenomena have also been observed for other folate-drug conjugates in mice, such as folate-mitomycin (1 min plasma half life; ref. 28) and  $^{99\text{m}}\text{Tc}$ -EC20 (4 min plasma half life; ref. 25); thus, the characteristics of EC145 seem to be representative for this class of targeted small molecules. Overall, EC145 seems to be a potent, folate-targeted chemotherapeutic that displays significant efficacy and tolerability in multiple FR-positive models. These exciting preclinical qualities have warranted the continued study of this molecule as well as provided justification for the start of EC145's Phase 1 clinical trial back in March 2006. Because the screening of a wide variety of human cancers has detected elevated functional FR expression levels on ovarian, renal, endometrial, lung, and breast cancers (27), EC145 may find itself to be most efficacious against some of these important clinical targets.

## Acknowledgments

Received 1/4/2007; revised 2/15/2007; accepted 2/21/2007.

**Grant support:** Grant 511040805 from the Indiana 21st Century Fund.

The costs of publication of this article were defrayed in part by the payment of page charges. This article must therefore be hereby marked *advertisement* in accordance with 18 U.S.C. Section 1734 solely to indicate this fact.

We thank Dr. Philip S. Low for his valuable comments, Dr. Alberto Gabizon for the J6456 and M109 cell lines, and Dr. Paul Snyder for the cryosectioning of tumor tissue.

## References

- Damle NK, Frost P. Antibody-targeted chemotherapy with immunoconjugates of calicheamicin. *Curr Opin Pharmacol* 2003;3:386-90.
- Giles F, Estey E, O'Brien S. Gemtuzumab ozogamicin in the treatment of acute myeloid leukemia. *Cancer* 2003;98:2095-104.
- Schrama D, Reisfeld RA, Becker JC. Antibody targeted drugs as cancer therapeutics. *Nat Rev Drug Discov* 2006; 5:147-59.
- Ross HJ, Hart LL, Swanson PM, et al. A randomized, multicenter study to determine the safety and efficacy of the immunoconjugate SGN-15 plus docetaxel for the treatment of non-small cell lung carcinoma. *Lung Cancer (Amsterdam, Netherlands)* 2006;54:69-77.
- Jain RK. Delivery of molecular and cellular medicine to solid tumors. *Adv Drug Deliv Rev* 2001;46:149-68.
- Reddy JA, Allagadda VM, Leamon CP. Targeting therapeutic and imaging agents to folate receptor positive tumors. *Curr Pharm Biotechnol* 2005;6: 131-50.
- Reddy JA, Low PS. Folate-mediated targeting of therapeutic and imaging agents to cancers. *Crit Rev Ther Drug Carrier Syst* 1998;15:587-627.
- Leamon CP, Low PS. Folate-mediated targeting: from diagnostics to drug and gene delivery. *Drug Discov Today* 2001;6:44-51.
- Reddy JA, Leamon CP, Low PS. Folate-mediated delivery of protein and peptide drugs into tumors. In: Torchilin V, editor. *Delivery of protein and peptide drugs in cancer*: World Scientific/Imperial College Press; 2006. p. 183-204.
- Low PS, Antony AC. Folate receptor-targeted drugs for cancer and inflammatory diseases. *Adv Drug Deliv Rev* 2004;56:1055-231.
- Weitman SD, Lark RH, Coney LR, et al. Distribution of the folate receptor GP38 in normal and malignant cell lines and tissues. *Cancer Res* 1992;52:3396-401.
- Ross JF, Chaudhuri PK, Ratnam M. Differential regulation of folate receptor isoforms in normal and malignant tissues *in vivo* and in established cell lines. Physiologic and clinical implications. *Cancer* 1994;73: 2432-43.
- Toffoli G, Cernigoi C, Russo A, Gallo A, Bagnoli M, Boiocchi M. Overexpression of folate binding protein in ovarian cancers. *Int J Cancer* 1997;74:193-8.
- Leamon CP, Low PS. Delivery of macromolecules into living cells: a method that exploits folate receptor endocytosis. *Proc Natl Acad Sci U S A* 1991;88:5772-6.
- Leamon CP, Low PS. Membrane folate-binding proteins are responsible for folate-protein conjugate endocytosis into cultured cells. *Biochem J* 1993;291: 855-60.
- Rund LA, Cho BK, Manning TC, Holler PD, Roy EJ, Kranz DM. Bispecific agents target endogenous murine T cells against human tumor xenografts. *Int J Cancer* 1999;83:141-9.
- Lu Y, Low PS. Folate targeting of haptens to cancer cell surfaces mediates immunotherapy of syngeneic murine tumors. *Cancer Immunol Immunother* 2002;51: 153-62.
- Lee RJ, Low PS. Delivery of liposomes into cultured KB cells via folate receptor-mediated endocytosis. *J Biol Chem* 1994;269:3198-204.
- Reddy JA, Abburi C, Hofland H, et al. Folate-targeted, cationic liposome-mediated gene transfer into disseminated peritoneal tumors. *Gene Ther* 2002; 9:1542-50.
- Reddy JA, Xu LC, Parker N, Vetzal M, Leamon CP. Preclinical evaluation of  $(^{99\text{m}}\text{Tc})$ -EC20 for imaging folate receptor-positive tumors. *J Nucl Med* 2004;45: 857-66.
- Ladino CA, Chari RV, Bourret LA, Kedersha NL, Goldmacher VS. Folate-maytansinoids: target-selective



- drugs of low molecular weight. *Int J Cancer* 1997;73:859-64.
22. Reddy JA, Westrick E, Vlahov I, Howard SJ, Santhapuram HK, Leamon CP. Folate receptor specific anti-tumor activity of folate-mitomycin conjugates. *Cancer Chemother Pharmacol* 2006;58:229-36.
23. Xu L, Vlahov IR, Leamon CP, Santhapuram HKR, Li CH. inventors; Endocyte, Inc., assignee. Synthesis and purification of pteric acid and conjugates thereof. USA. 2006.
24. Vlahov IR, Santhapuram HK, Kleindl PJ, Howard SJ, Stanford KM, Leamon CP. Design and regioselective synthesis of a new generation of targeted chemotherapeutics. Part 1: EC145, a folic acid conjugate of desacetylvinblastine monohydrazone. *Bioorg Med Chem Lett* 2006;16:5093-6.
25. Leamon CP, Parker MA, Vlahov IR, et al. Synthesis and biological evaluation of EC20: a new folate-derived, (99m)Tc-based radiopharmaceutical. *Bioconjug Chem* 2002;13:1200-10.
26. Mathias CJ, Wang S, Lee RJ, Waters DJ, Low PS, Green MA. Tumor-selective radiopharmaceutical targeting via receptor-mediated endocytosis of gallium-67-deferoxamine-folate. *J Nucl Med* 1996;37:1003-8.
27. Parker N, Turk MJ, Westrick E, Lewis JD, Low PS, Leamon CP. Folate receptor expression in carcinomas and normal tissues determined by a quantitative radioligand binding assay. *Anal Biochem* 2005;338:284-93.
28. Leamon CP, Reddy JA, Vlahov IR, et al. Synthesis and biological evaluation of EC72: a new folate-targeted chemotherapeutic. *Bioconjug Chem* 2005;16:803-11.
29. Naveed F, Fisher R, Engel JS, Lu J, Low PS, Amato RJ. Folate-scan in subjects with suspected metastatic renal cell carcinoma. 2004 ASCO Annual Meeting Proceedings. *J Clin Oncol* 2004;4751.